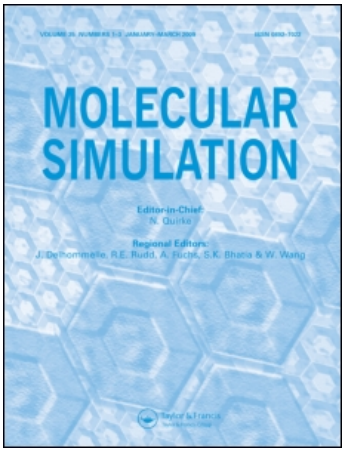

Molecular Simulation
Publication details, including instructions for authors and subscription information:
http://www.informaworld.com/smpp/title~content=t713644482

Comparison of Different Three-site Interaction Potentials for Liquid Acetonitrile

E. Guàrdia[a]; R. Pinzón[a]; J. Casulleras[a]; M. Orozco[b]; F. J. Luque[c]
[a] Departament de Física i Enginyeria Nuclear, Universitat Politècnica de Catalunya, Barcelona, Spain [b] Departament de Bioquímica i Biologia Molecular, Universitat de Barcelona, Barcelona, Spain [c] Departament de Físicoquímica, Universitat de Barcelona, Barcelona, Spain

To cite this Article Guàrdia, E. , Pinzón, R. , Casulleras, J. , Orozco, M. and Luque, F. J.(2001) 'Comparison of Different Three-site Interaction Potentials for Liquid Acetonitrile', Molecular Simulation, 26: 4, 287 — 306
To link to this Article: DOI: 10.1080/08927020108024509
URL: http://dx.doi.org/10.1080/08927020108024509

Molecular Simulation, 2001, Vol. 26, pp. 287–306
Reprints available directly from the publisher
Photocopying permitted by license only

COMPARISON OF DIFFERENT THREE-SITE INTERACTION POTENTIALS FOR LIQUID ACETONITRILE

E. GUÀRDIA[a,*], R. PINZÓN[a], J. CASULLERAS[a], M. OROZCO[b] and F. J. LUQUE[c]

[a]*Departament de Física i Enginyeria Nuclear, Universitat Politècnica de Catalunya, Sor Eulàlia d'Anzizu s.n., B4-B5, 08034, Barcelona. Spain;* [b]*Departament de Bioquímica i Biologia Molecular, Universitat de Barcelona, Martí i Franquès 1, 08028, Barcelona. Spain;* [c]*Departament de Físicoquímica, Universitat de Barcelona, Diagonal s.n., 08028, Barcelona. Spain*

(Received June 2000; accepted June 2000)

Computer simulations of liquid acetonitrile at normal room conditions are reported. Both static and dynamic properties are analysed. Special attention is paid to the dielectric properties. A three-site interaction potential has been derived from *ab initio* calculations on the gas phase dimer and a comparison with different three-site interaction potentials available in the literature is presented. The suitability of three-site models to reproduce the properties of the real liquid is discussed by comparing computer simulation results with experimental data.

Keywords: Liquid acetonitrile; Three-site models; Structure; Dynamics; Dielectric properties

1. INTRODUCTION

Acetonitrile is a dipolar liquid with a simple molecular structure and high symmetry which is often used as an aprotic solvent in organic and electroorganic chemistry. Most of the computer simulation studies so far reported for acetonitrile and acetonitrile solutions are based on the assumption of rigid molecular models that do not consider explicitly the hydrogen atoms of the methyl group. With this assumption, the computing time is significantly reduced and longer simulations of larger systems can be

*Corresponding author.

carried out. In the last few years, three-site interaction potentials have been used to study solvation dynamics in acetonitrile [1, 2] and the conformation of biomolecules in acetonitrile solutions [3].

The potential proposed by Edwards *et al.* [4] and the OPLS potential of Jorgensen and Briggs [5] are the three-site interaction potentials most widely used for acetonitrile. The potential of Edwards *et al.* [4] is an empirical potential with the partial charges chosen simply to reproduce the dipole and quadrupole moments corresponding to the six-site model of Böhm and co-workers [6] and consequently the thermodynamic results were not optimized. The OPLS potential was obtained from *ab initio* calculations on the acetonitrile–water dimer. Although it reproduces reasonably well the structure and thermodynamic properties of liquid acetonitrile [5, 7], it gives a dielectric constant which is significantly smaller than the experimental one, as it has been recently shown [8]. In this paper we derive a three-site interaction potential from *ab initio* calculations on the acetonitrile–acetonitrile dimer. We perform computer simulations using the *ab initio*, the OPLS and the Edwards *et al.*, potentials. Such simulations are carried out in order to test the adequacy of three-site models to reproduce the properties of the real liquid. Both static and dynamic properties are analysed. Since this work is part of a project concerned with the study of ionic association in liquid acetonitrile, we pay special attention to the dielectric properties. The study of dielectric properties of liquids by computer simulation is still a major challenge, due to the extremely long trajectories required in order to obtain adequate statistical accuracy for collective properties such us the static dielectric constant ε_0 and the Debye relaxation time τ_D.

The organization of this paper is as follows: In Section 2, we describe the interaction potential models and the details of the simulations. In Section 3 we discuss the thermodynamic properties of the liquid. The structure and single particle dynamics are discussed in Sections 4 and 5, respectively. Section 6 is devoted to the analysis of dielectric properties. Finally, some concluding remarks are presented in Section 7.

2. INTERACTION POTENTIALS AND COMPUTER SIMULATION DETAILS

The acetonitrile monomer was represented by three interaction sites: the methyl group Me centered on carbon, and the carbon C and nitrogen N atoms. We adopted the same bond lengths as Jorgensen and Briggs [5], *i.e.*,

$r_{MeC} = 1.458$ Å and $r_{CN} = 1.157$ Å. The interaction energy between two molecules a and b was represented by

$$U_{ab}(r_{ij}) = \sum_i \sum_j \left[\frac{A_i A_j}{r_{ij}^{12}} - \frac{C_i C_j}{r_{ij}^{6}} + \frac{q_i q_j}{r_{ij}} \right] \quad (1)$$

where r_{ij} is the distance between site i of molecule a and site j of molecule b. The coefficients of the short range part can be expressed in terms of Lennard-Jones parameters, $A_i^2 = 4\varepsilon_i \sigma_i^{12}$ and $C_i^2 = 4\varepsilon_i \sigma_i^6$, and q_i is the charge assigned to site i.

To determine the interaction potential parameters, *ab initio* calculations were performed for the acetonitrile–acetonitrile dimer. The partial charges q_i were determined by fitting the *ab initio* calculations to quantum mechanical molecular electrostatic potentials [9]. The experimental gas phase dipole moment (3.91 D [10]) was introduced as a constraint in the fits. Electrostatic potentials and charges were evaluated by using the MOPETE/MOPFIT programs [11]. In all cases, the 6–31G** basis set was used and the wave functions were determined with the GAUSSIAN-94 package [12]. Lennard-Jones parameters were determined by fitting classical and quantum interaction energies for different configurations of the dimer. The OPLS parameters were initially assumed. Five different orientations were considered and for each orientation ten separations were analysed, ranging from 2 Å to 10 Å. Interaction energies and geometries were determined at the HF/6–31G** level using GAUSSIAN-94. In the last stage of the parameterization process, the HF-optimized Lennard-Jones parameters were still refined by fitting Monte Carlo estimates to the experimental liquid density. The final parameters and partial charges are listed in Table I.

To determine the thermodynamic properties of the *ab initio* model we performed a Monte Carlo simulation in the isothermal–isobaric NPT ensemble. The number of molecules was $N = 268$ and the usual periodic

TABLE I Parameters of the interaction potentials and molecular dipole moments

Model	*Site*	$\varepsilon/kJmol^{-1}$	$\sigma/Å$	q/e	μ/D
Ab initio	Me	0.7824	3.775	0.206	3.96
	C	0.544	3.650	0.247	
	N	0.6276	3.200	−0.453	
OPLS [5]	Me	0.866	3.775	0.15	3.44
	C	0.628	3.650	0.28	
	N	0.711	3.200	−0.43	
Edwards *et al.* [4]	Me	1.586	3.6	0.269	4.12
	C	0.416	3.4	0.129	
	N	0.416	3.3	−0.398	

boundary conditions were assumed. The pressure was fixed at 1 atm and the temperature at 298 K. We used a molecular based spherical cut-off at 10 Å. The equilibration period consisted of 2×10^6 configurations and the production period of 3×10^6 configurations.

Three MD simulations were carried out, using the *ab initio*, the OPLS and the Edwards *et al.*, models, respectively. The corresponding interaction potential parameters and molecular dipole moments are collected in Table I. In the case of the interaction potential of Edwards *et al.*, the intramolecular distances are $r_{MeC} = 1.46$ Å and $r_{CN} = 1.17$ Å, and the Lorentz-Berthelot combining rules were assumed [13]. In the case of the MD runs we considered a system made up of $N = 216$ molecules at the experimental density (see Tab. II). The temperature was kept at $T = 298$ K by using the integration algorithm proposed by Berendsen *et al.* [14]. Bond lengths were kept fixed during the simulations by using the SHAKE method [15]. To handle with the long-range coulombic interactions we used the Ewald summation technique with conducting boundary conditions [16]. We employed a timestep of 0.01 ps. Each run consisted of an initial equilibration period of 50 ps and a production period of 1000 ps.

3. THERMODYNAMICS

The thermodynamic properties resulting from the Monte Carlo simulation with the *ab initio* model are compared in Table II with the results reported by Jorgensen and Briggs for the OPLS potential [5] and with experimental data. The calculated density d clearly improves that resulting from the OPLS model although it is still too low and correspondingly the volume per molecule V is a little high.

The heat of vaporization ΔH_{vap} was calculated as

$$\Delta H_{vap} = -U + RT - (H^0 - H) \tag{2}$$

TABLE II Thermodynamic properties

	Ab initio model	*OPLS model* [a]	*Exptl*
d/kg m^{-3}	770 ± 1	765 ± 2	777 ± 2 [17]
V/Å^3	88.4 ± 0.1	89.1 ± 0.2	87.7 ± 2 [17]
$-U$/kJ mol^{-1}	32.63 ± 0.04	31.2 ± 0.1	31.0 ± 0.2 [18]
ΔH^0_{vap}/kJ mol^{-1}	35.14 ± 0.08	33.6 ± 0.1	33.5 ± 0.2 [18]
$10^{11}\kappa$/Pa^{-1}	75 ± 8	64 ± 6	81.7 [19]
C_p/J mol^{-1} K^{-1}	92 ± 6	81 ± 3	91.6 [20]

[a] From Ref. [5].

where U is the intermolecular energy of the liquid and $H^0 - H$ is the enthalpy difference between the real and ideal was. At 298 K, it is $H^0 - H = 0.5 \pm 0.2$ kJ mol^{-1} [18]. As can be seen in Table II, both $-U$ and ΔH_{vap} are slightly higher than the experimental values. These thermodynamic properties are very well reproduced by the OPLS model. On the other hand, the intermolecular energy reported for the potential of Edwards *et al.*, $-U = 34.2$ kJ mol^{-1} [4], is in worse agreement with experiments than that obtained with the *ab initio* model.

The isothermal compressibility κ and the intermolecular contribution to the heat capacity ΔC_p were computed from the fluctuation formulas

$$\kappa = \frac{\langle V^2 \rangle - \langle V \rangle^2}{k_B T \langle V, \rangle}, \tag{3}$$

$$\Delta C_p = \frac{\langle H^2 \rangle - \langle H \rangle^2}{N k_B T^2}. \tag{4}$$

In order to be compared with the experimental C_p, the computed ΔC_p value needs to be augmented by the unimolecular contribution which may be approximated as C_p for the ideal gas less R and amounts to 43.9 J mol^{-1} K^{-1} [20]. Although the convergence is slower and the statistical uncertainty is greater than for the other thermodynamic properties (see Tab. II), the improvement with respect to the OPLS results is evident and in the particular case of C_p the experimental value is almost reproduced.

4. STRUCTURE

The site–site radial distribution functions $g_{ij}(r)$ computed from the MD simulations are presented in Figure 1. All the models exhibit the same structural features which are consistent with the results obtained by Böhm *et al.* [6] using a six-site model. In general, the *ab initio* potential results are very close to those obtained with the OPLS model and they show some minor discrepancies with respect to the $g_{ij}(r)$ resulting from the model of Edwards *et al.* Our findings are in very good agreement with previous computer simulation results using the OPLS [5, 7] and the Edwards *et al.*, models [21], respectively.

In order to test the adequacy of the interaction potentials to account for the structure of the real liquid, comparison is made with experimental structure factors. Since we are using molecular models that do not consider explicitly the hydrogen atoms of the methyl group, X-ray results are more

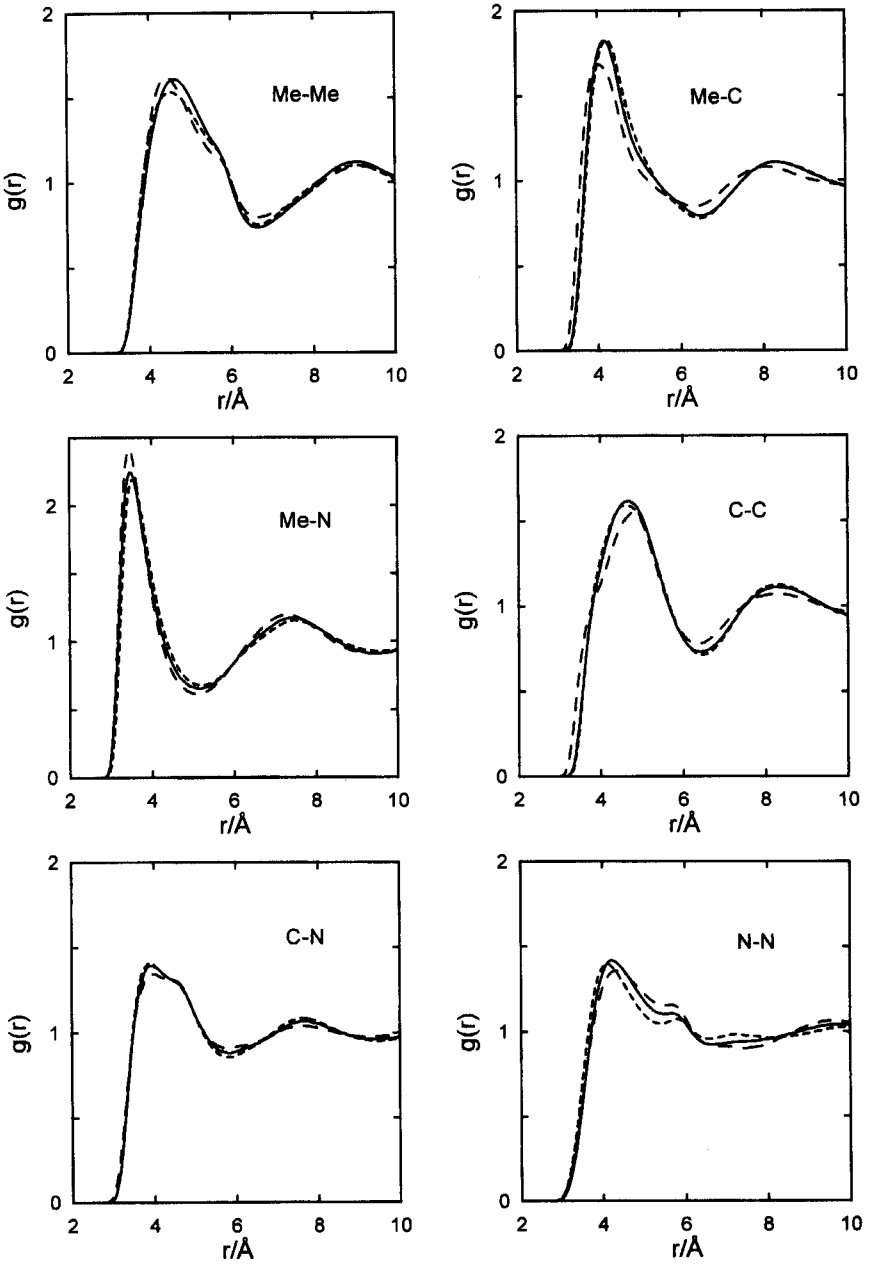

FIGURE 1 Site–site radial distribution functions. —— *ab initio* model, - - - - OPLS model, – – – – Edwards *et al.*, model.

appropriate than neutron-diffraction data. The intermolecular structure factor obtained from X-ray scattering by Radnai and co-workers [7, 22] was reported in terms of the function

$$kH(k) = k \sum_i \sum_j x_i x_j f_i(k) f_j(k) (A_{ij}(k) - 1) M(k) \tag{5}$$

where x_i is the atomic fraction of the atom or atomic group i and $f_i(k)$ is the related coherent scattering factor [7, 22]. The scattering factors were taken from Ref. [23] in the case of the Me group, and from Ref. [24] in the case of

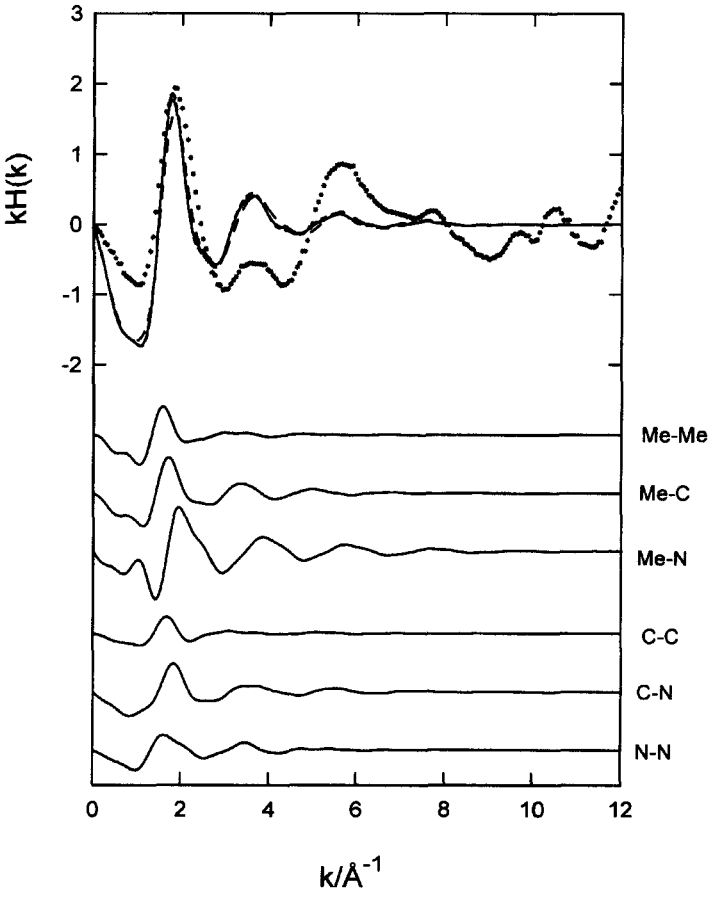

FIGURE 2 Intermolecular structure resulting from X-ray measurements (* * *) compared with MD results (—— *ab initio* model, - - - - OPLS model, – – – – Edwards *et al.*, model). The partial contributions to $kH(k)$ obtained by computer simulation with the *ab initio* model are also represented (the origin of these curves is vertically displaced).

the N and C atoms. The partial structure functions $A_{ij}(k)$ are the Fourier transforms of the site–site radial distribution functions $g_{ij}(r)$,

$$A_{ij}(k) = 1 + \frac{4\pi\rho}{k}\int_0^\infty r(g_{ij}(r) - 1)\sin(kr)dr \tag{6}$$

where ρ is the molecular number density and $M(k)$ is a modification function which has the form

$$M(k) = \frac{1}{\sum_i (x_i f_i)^2}\exp(-\beta k^2) \tag{7}$$

and $\beta = 0.01\,\text{Å}^2$ is a damping factor. The $kH(k)$ functions resulting from MD for the different interaction potentials are almost identical, as can be seen in Figure 2. Only some small differences in the height of the first peak at $1.8\,\text{Å}^{-1}$ are appreciated. In the case of the *ab initio* model, the six partial contributions to $kH(k)$ are also shown in Figure 2. Although all the partials contribute to the first peak of $kH(k)$, the more important contributions are those involving the Me group. The secondary peaks shown at $3.6\,\text{Å}^{-1}$ and $5.6\,\text{Å}^{-1}$ are mainly determined for the partials involving the N atom. The MD simulations reproduce fairly well the position and height of the first peak of the $kH(k)$ function obtained from X-ray scattering. Although the positions of the secondary peaks are also reproduced, in this case the agreement is less satisfactory. Nevertheless, one should note that the resolution of X-ray experiments is lower at high k values.

5. DYNAMICS

The normalized velocity autocorrelation functions $C_v(t)$ corresponding to the Me group, the C atom and the N atom were determined from the MD simulations. Figure 3 shows the $C_v(t)$ functions obtained for the *ab initio* model. The results do not differ appreciably from those resulting with the other interaction potentials. The $C_v(t)$ functions show the oscillatory shape characteristic of dense liquids. The oscillations are less pronounced for the central C atom. The corresponding power spectra $S_v(\omega)$ were obtained as the Fourier transforms, *i.e.*,

$$S_v(\omega) = \int_0^\infty C_v(t)\cos\omega t dt. \tag{8}$$

For the C and N atoms we observe peaks centered at $30\,\text{cm}^{-1}$ and at $45\,\text{cm}^{-1}$, respectively. In the case of the Me group, $S_v(\omega)$ exhibits a broader

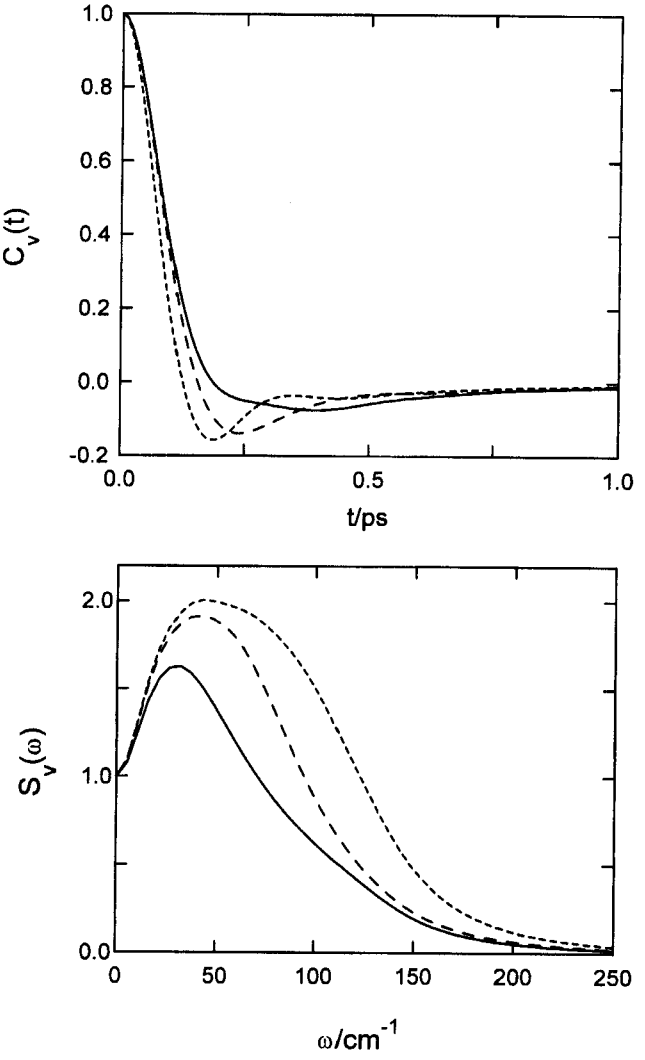

FIGURE 3 Atomic velocity autocorrelation functions and power spectra for the *ab initio* model. - - - - Me group, —— C atom, – – – – N atom.

peak and the central position is not so well defined. These low frequency peaks are characteristic of dense liquids and they are due to translational vibrations of the molecules inside the cage formed by their neighbours.

The molecular self-diffusion coefficient D was determined from the long time slope of the centre of mass mean square displacement $r^2_{CM}(t)$. The $r^2_{CM}(t)$ functions for the different models are shown in Figure 4 and the D

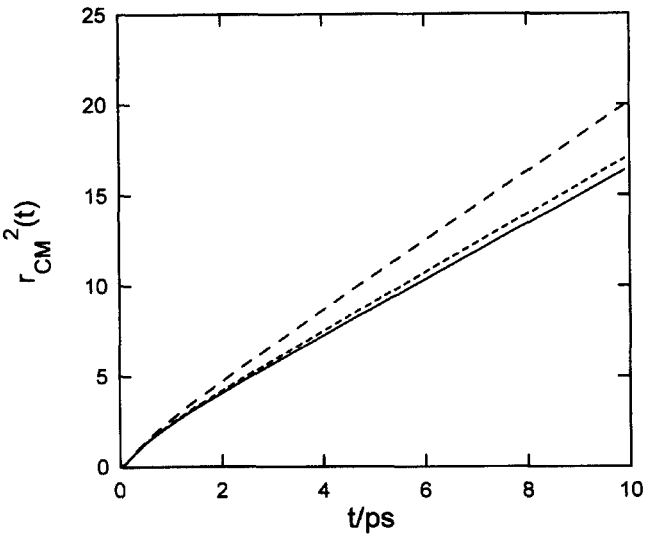

FIGURE 4 Centre of mass mean square displacement in units of $Å^2$. —— *ab initio* model, - - - - OPLS model, – – – – Edwards *et al.*, model.

values are given in Table III. For the *ab initio* and the OPLS models we obtain a very similar result while the model of Edwards *et al.*, exhibits a slightly higher mobility. All the models give D values which are lower than the experimental data resulting either from NMR [25] or from quasielastic neutron diffraction scattering [26].

Reorientational motions in liquids are usually studied through a set of time dependent correlation functions $C_l(t)$ defined as

$$C_l(t) = \langle P_l(\vec{u}(t) \cdot \vec{u}(0)) \rangle \tag{9}$$

where P_l refers to the l th Legendre polynomial and $\vec{u}$ is a unitary vector that characterizes the orientation of the molecule. Reorientational correlation times are then calculated by assuming an exponential decay of $C_l(t)$ at long times, *i.e.*,

$$C_l(t) = \exp(-t/\tau_l). \tag{10}$$

TABLE III Self-diffusion coefficients and molecular reorientational times

	Ab initio model	*OPLS model*	*Edwards et al., model*	*Exptl*
$D/10^{-9}\,m^2s$	2.6	2.7	3.1	4.04 [25], 4.2 [26]
τ_1/ps	3.8	3.55	3.9	3.28 [28], 3.68 [29]
τ_2/ps	1.60	1.45	1.55	1.02 [25]

We considered the unit vector in the direction of the molecular axis and we calculated the reorientational correlation functions for $l=1$ and $l=2$ which describe the tumbling motion of the acetonitrile molecule [27]. The $C_l(t)$ functions obtained for the different interaction potentials are shown in Figure 5 and the τ_l values are given in Table III. Although we do not find any difference in the short time reorientational motion, at intermediate and long times a clear trend is observed, *i.e.*, the higher the molecular dipole moment, the slower the reorientation. All the models give τ_l values that are slightly larger than the data resulting from Raman [28] and infrared [29] band shapes and from NMR [25] experiments.

According to our findings, a common defect of the different three-site interaction potentials for acetonitrile is that they lead to a dynamics which is slower than that observed in the real liquid. The disagreement is specially significant in the case of the translational motion. On the other hand, with the six site model of Böhm *et al.* [27] the experimental D and τ_l values were almost reproduced. We could then conclude that it should be necessary to consider explicitly the hydrogen atoms of the Me group in order to improve the single particle dynamics.

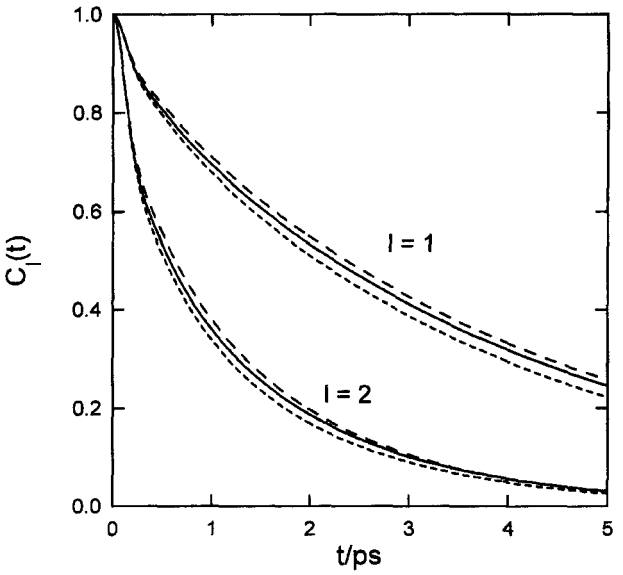

FIGURE 5 Reorientational correlation functions. —— *ab initio* model, - - - - OPLS model, – – – – Edwards *et al.*, model.

6. DIELECTRIC PROPERTIES

For a system with long-range interactions treated by the Ewald method with conducting boundary conditions, the static dielectric constant ε_0 is given by [30]

$$\varepsilon_0 = \varepsilon_\infty + 3yG_k \tag{11}$$

where ε_∞ is the dielectric constant at optical frequencies, $y = 4\pi\rho\mu^2/9K_BT$ is the dimensionless dipolar strength and G_k is the finite system Kirkwood g factor

$$G_k = \frac{\langle M^2 \rangle}{N\mu^2} \tag{12}$$

which measures the equilibrium fluctuations of the total dipole moment of the sample $\vec{M} = \sum_{i=1}^{N} \vec{\mu}_i$. Because we are assuming rigid non-polarizable molecules, in the case of the MD simulations it is $\varepsilon_\infty = 1$. Once ε_0 has been obtained from Eq. (11), the Kirkwood factor g_k which describes orientational correlations in an infinite sample may be calculated by means of the relationship

$$g_k = \frac{2\varepsilon_0 + \varepsilon_\infty}{3\varepsilon_0} G_k. \tag{13}$$

The values of G_k, ε_0 and g_k found in this way are given in Table IV. The indicated errors were determined with the blocking method of Ref. [31]. Our results for the OPLS and Edwards *et al.*, models are in close agreement with those reported by Mountain, $\varepsilon_0 = 18 \pm 1$ and $\varepsilon_0 = 28 \pm 1$, respectively [8]. The ε_0 value obtained with the *ab initio* potential clearly improves that resulting from the OPLS model, and it approaches that computed by using the model of Edwards *et al.* Nevertheless, both *ab initio* and Edwards *et al.*, models give a static dielectric constant which is a little low compared with the value

TABLE IV Dielectric properties

	Ab initio model	*OPLS model*	*Edwards et al., model*	*Exptl* [32]
G_k	1.37 ± 0.05	1.22 ± 0.03	1.48 ± 0.06	
y	6.07	4.58	6.57	
ε_0	26.2 ± 0.7r	17.5 ± 0.4	30.2 ± 0.9	35.84
$\varepsilon_0 - \varepsilon_\infty$	25.2	16.5	29.2	32.33
g_k	0.93	0.84	1.00	
τ_Φ/ps	3.4	2.7	4.4	
τ_D/ps	3.3	2.6	4.3	3.4
τ_D/τ_1	0.87	0.73	1.10	

obtained by Barthel and co-workers from dielectric relaxation measurements [32]. Since part of these discrepancies are due to the value of the high-frequency dielectric constant ε_∞ (the value reported by Barthel *et al.*, is $\varepsilon_\infty = 3.51$ [32]), we find more significant to compare the difference $\varepsilon_0 - \varepsilon_\infty$. Table IV shows that in this case the discrepancies are effectively reduced.

To get further insight into the model dependence of ε_0 we have analysed the radial decomposition of the Kirkwood factor $G_k(R)$, defined by

$$G_k(R) = \frac{1}{N\mu^2} \left\langle \sum_{r_{ij} \leq R} \vec{\mu}_i \cdot \vec{\mu}_j \right\rangle \tag{14}$$

Apart from a normalization factor, $G_k(R)$ is the average dipole moment of a sphere of radius R around a reference molecule. For $R \to \sqrt{3}/2L$ (L is the length of the simulation box), $G_k(R)$ tends to the values given in Table IV. $G_k(R)$ can be evaluated using

$$G_k(R) = 1 + \frac{4\pi\rho}{3} \int_0^R 3g_{CM}(r)\langle \cos\theta(r)\rangle r^2 dr \tag{15}$$

where $g_{CM}(r)$ is the centre of mass radial distribution function and $\theta(r)$ is the angle between the dipole moments of two molecules separated a distance r. Figure 6 shows that the qualitative behaviour is the same for the three

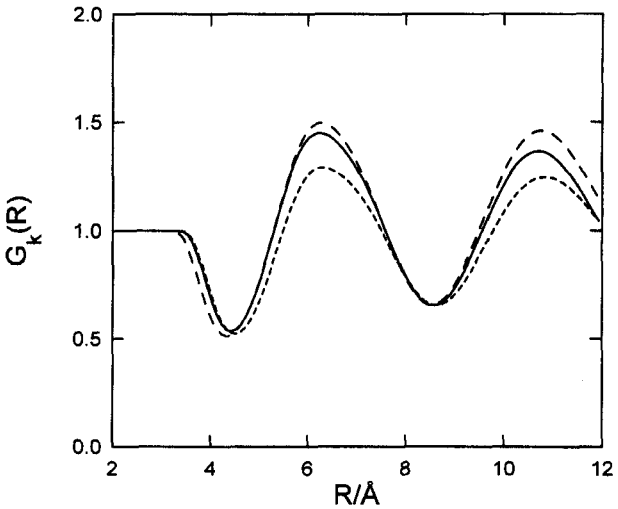

FIGURE 6 R-dependent finite system Kirkwood g factor. —— *ab initio* model, - - - - OPLS model, – – – – Edwards *et al.*, model.

models. The oscillatory shape of $G_k(R)$ indicates that there is an antiparallel arrangement of near neighbouring molecules. This feature was already observed in the pioneering work of Edwards and co-workers [4]. In the full R range, we observe that the degree of molecular ordering systematically increases as the molecular dipole moment increases.

The relaxation of the collective orientational ordering can be studied through the total dipole moment autocorrelation function

$$\Phi(t) = \frac{\langle \vec{M}(t) \cdot \vec{M}(0) \rangle}{\langle M^2(0) \rangle} \tag{16}$$

which is the collective analogue of the single particle reorientational function $C_1(t)$ (see Eq. (9)). The functions $\Phi(t)$ obtained for the different models are shown in Figure 7. It is interesting to consider the short time behaviour. For acetonitrile we do not see the oscillatory "libration" characteristic of strongly associated H-bonded liquids such us water [34, 35] and methanol [36]. Instead of that, we observe a nearly Gaussian initial decay, similar to that found for liquid chloroform [37]. The collective

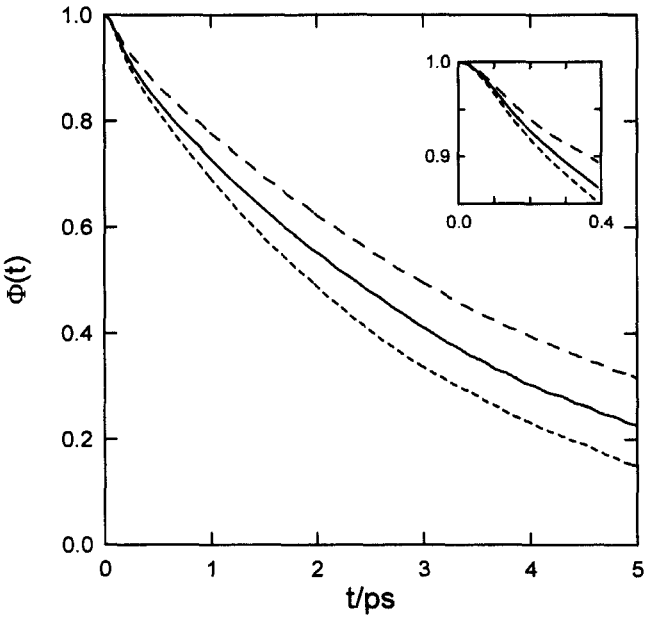

FIGURE 7 Total dipole moment autocorrelation functions. —— *ab initio* model, - - - - OPLS model, – – – – Edwards *et al.*, model. The insert shows the short time behaviour of the $\Phi(t)$ functions.

analogue of the single particle reorientational time can be determined by fitting an exponential function to $\Phi(t)$, *i.e.*, at long times

$$\Phi(t) = \exp(-t/\tau_\Phi). \tag{17}$$

As can be seen from Table IV, τ_Φ increases as the molecular dipole moment increases. The influence of the assumed model is significantly more important for τ_Φ than for τ_1 (see Tab. III).

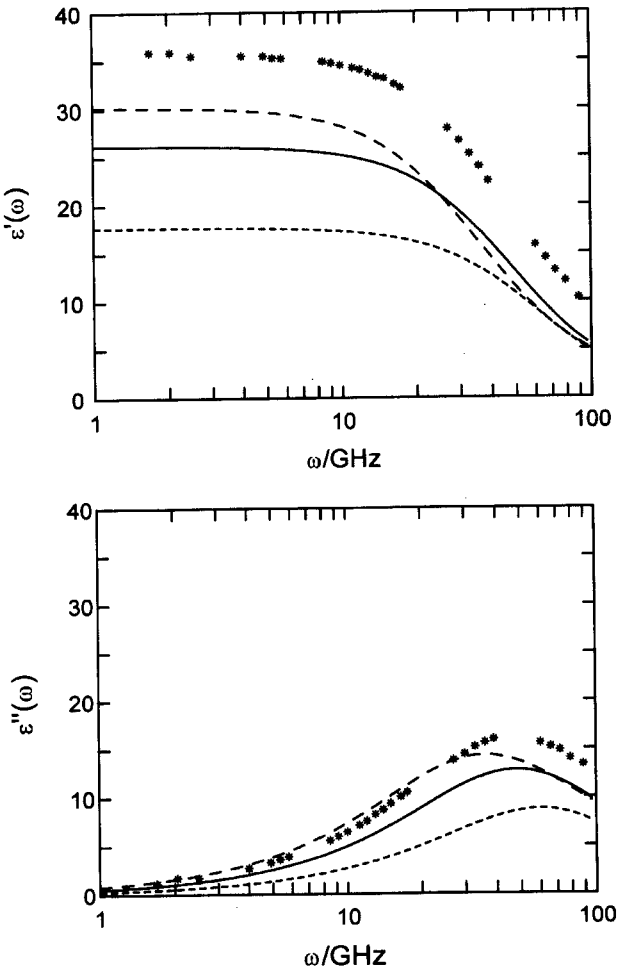

FIGURE 8 Frequency dependent dielectric constant. —— *ab initio* model, - - - - OPLS model, – – – – Edwards *et al.*, *model*, * * * experimental data [32].

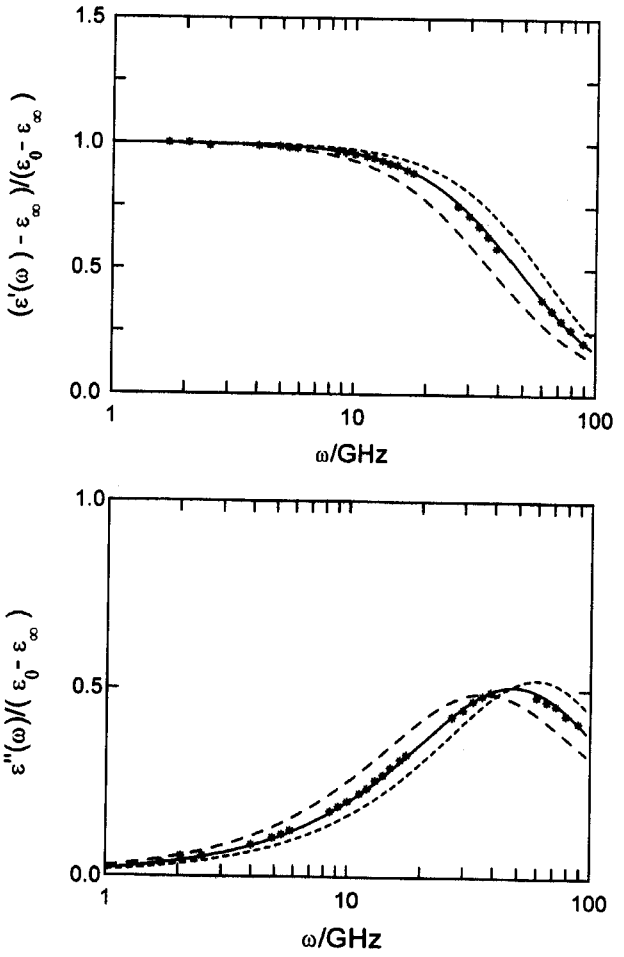

FIGURE 9 Same as Figure 8 with the real and imaginary parts of the frequency dependent dielectric constant scaled as $(\varepsilon'(\omega)-\varepsilon_\infty)/(\varepsilon_0-\varepsilon_\infty)$ and $\varepsilon''(\omega)/(\varepsilon_0-\varepsilon_\infty)$, respectively.

The real and imaginary parts of the frequency-dependent dielectric constant $\varepsilon(\omega)=\varepsilon'(\omega)-i\varepsilon''(\omega)$ are given by [33, 34]

$$\varepsilon'(\omega) = \varepsilon_0 - (\varepsilon_0 - \varepsilon_\infty)\omega \int_0^\infty \Phi(t) \sin \omega t dt, \tag{18}$$

$$\varepsilon''(\omega) = (\varepsilon_0 - \varepsilon_\infty)\omega \int_0^\infty \Phi(t) \cos \omega t dt. \tag{19}$$

Once $\varepsilon(\omega)$ has been obtained, the so-called Debye relaxation time may be determined from the low-frequency behaviour,

$$\tau_D = \lim_{\omega \to 0} \frac{\varepsilon_0 - \varepsilon(\omega)}{i\omega(\varepsilon(\omega) - \varepsilon_\infty)}. \tag{20}$$

Since dielectric relaxation of acetonitrile is dominated by one single process [32], τ_D should be essentially identical to τ_Φ. As shown in Table IV, it is $\tau_D \simeq \tau_\Phi$ for all the models (we estimate a statistical uncertainty of approximately 5% in the reported values). The calculated τ_D value for the *ab initio* model is in very good agreement with the experimental dielectric relaxation time, whereas the values for the OPLS and Edwards *et al.*, models are clearly too low and too high, respectively. On the other hand, the relation between the total and single particle relaxation times is important from a theoretical point of view (see, for instance, Ref. [38]). For all the models, we find $\tau_D/\tau_1 \simeq g_k$. The same relationship was obtained by Neumann for liquid water [34].

The MD results for $\varepsilon'(\omega)$ and $\varepsilon''(\omega)$ are compared with the experimental findings of Barthel *et al.* [32] in Figure 8. The dependence of the permittivity with frequency is qualitatively reproduced by the MD simulations, although some quantitative disagreements can be observed. These disagreements are partly due to the discrepancies in the values of ε_0 and ε_∞. In Figure 9, this is overcome by plotting the quantities $(\varepsilon'(\omega)-\varepsilon_\infty)/(\varepsilon_0-\varepsilon_\infty)$ and $\varepsilon''(\omega)/(\varepsilon_0-\varepsilon_\infty)$. These scaled functions are mainly determined by the dielectric relaxation time τ_D and, in accordance with the discussion given above, the *ab initio* model fits very well the experimental curves. For the other models, we still observe some discrepancies in the decay of the $(\varepsilon'(\omega)-\varepsilon_\infty)/(\varepsilon_0-\varepsilon_\infty)$ function as well as in the position of the peak of $\varepsilon''(\omega)/(\varepsilon_0-\varepsilon_\infty)$.

7. CONCLUDING REMARKS

The *ab initio* potential for acetonitrile derived in this work reproduces fairly well a variety of experimental properties of liquid acetonitrile, including thermodynamic, X-ray and dielectric relaxation data. The agreement is not so satisfactory in the case of the single particle dynamics and we obtain a self-diffusion coefficient significantly slower than that corresponding to the real liquid. The same deficiency is observed when the other three-site interaction potentials are assumed. The *ab initio* potential clearly improves the thermodynamic and dielectric properties resulting from the OPLS

model. Both *ab initio* and Edwards *et al.*, models give results for the static dielectric constant in reasonable agreement with the experimental data. The agreement is slightly closer in the case of the potential of Edwards *et al.* The *ab initio* model also reproduces the experimental dielectric relaxation time whereas for the potential of Edwards *et al.*, a too high value is obtained.

The comparison among the results obtained with the different interaction potentials shows the influence of the assumed model on the different properties. Although the structure and the short time dynamics are not very sensitive to the assumed interaction potential, major differences appear when the long time dynamics and dielectric properties are considered. We observe that both the static dielectric constant and the Debye relaxation time systematically increase as the molecular dipole moment increases. We think this is an important conclusion that should be taken into account when deriving interaction potentials explicitly including molecular polarizability.

Acknowledgements

We thank Dr. R. Buchner for helpful discussions. R. P. gratefully acknowledges a fellowship from "Instituto de Cooperación Iberoamericana". This work has been supported by the Spanish "Ministerio de Educación y Cultura" (TIC95-0429 and PB96-0170-CO3 Grants) and the "Generalitat de Catalunya" (1999SGR-00146 Grant). The *ab initio* calculations were performed at the CESCA (Centre de Supercomputació de Catalunya).

References

[1] Maroncelli, M. (1991). "Computer simulations of solvation dynamics in acetonitrile", *J. Chem. Phys.*, **94**, 2084.
[2] Ladanyi, B. M. and Klein, S. (1996). "Contributions of rotation and translation to polarizability anisotropy and solvation dynamics in acetonitrile", *J. Chem. Phys.*, **105**, 1552.
[3] Troxler, L. and Wipff, G. (1994). "Conformation and dynamics of 18-crown-6, cryptand 222, and their cation complexes in acetonitrile studied by molecular dynamics simulations", *J. Am. Chem. Soc.*, **116**, 1468.
[4] Edwards, D. M. F., Madden, P. A. and McDonald, I. R. (1984). "A computer simulation study of the dielectric properties of a model of methyl cyanide. I. The rigid dipole case", *Mol. Phys.*, **51**, 1141.
[5] Jorgensen, W. L. and Briggs, J. M. (1988). "Monte Carlo simulations of liquid acetonitrile with a three-site model", *Mol. Phys.*, **63**, 547.
[6] Böhm, H. J., McDonald, I. R. and Madden, P. A. (1983). "An effective potential for acetonitrile", *Mol. Phys.*, **49**, 347.
[7] Radnai, T. and Jedlovszky, P. (1994). "Reverse Monte Carlo simulation of a heteronuclear molecular liquid: Structural study of acetonitrile", *J. Phys. Chem.*, **98**, 5994.
[8] Mountain, R. D. (1997). "Shear viscosity and dielectric constant of liquid acetonitrile", *J. Chem. Phys.*, **107**, 3921.

[9] Momany, F. A. (1978). "Determination of partial atomic charges from *ab initio* molecular electrostatic potentials. Application to formamide, methanol and formic acid", *J. Phys. Chem.*, **82**, 592.
[10] Gray, C. G. and Gubbins, K. E., *Theory of Molecular Liquids*, Clarendon Press, Oxford, 1984, Appendix D.
[11] Luque, F. J. and Orozco, M., *MOPETE/MOPFIT Computer programs*, University of Barcelona, 1998.
[12] Frichs, M. J., Trucks, G. W., Schlegel, H. B., Gill, P. M. W., Johnson, B. G., Robb, M. A., Cheeseman, J. R., Keith, T. A., Petersson, G. A., Montgomery, J. A., Raghavachari, K., Al-Laham, M. A., Zakrzewski, V. G., Ortiz, J. V., Foresman, J. B., Cioslowski, J., Stefanov, B. B., Nanayakkara, A., Challacombe, M., Peng, C. Y., Ayala, P. Y., Chen, W., Wong, M. W., Anfres, J. L., Reploge, E. S., Gomperts, R., Martin, R. L., Fox, D. J., Binkley, J. S., Defress, D. J., Baker, J., Stewart, J. J. P., Head-Gordon, M., Gonzalez, C. and Pople, J. A., *GAUSSIAN 94 (Rev. A.1)*, GAUSSIAN Inc., Pittsburgh, 1995.
[13] Hansen, J. P. and McDonald, I. R., *Theory of Simple Liquids*, Academic Press, London, 1986, Chapter 6.
[14] Berendsen, H. J. C., Postma, J. P. M., van Gunsteren, W. F., DiNola, A. and Haak, J. R. (1984). "Molecular dynamics with coupling to an external bath", *J. Chem. Phys.*, **81**, 3684.
[15] Ciccotti, G., Ferrario, M. and Ryckaert, J. P. (1982). "Molecular dynamics of rigid systems in cartesian coordinates. A general formulation", *Mol. Phys.*, **47**, 1253.
[16] Allen, M. P. and Tildesley, D. J., *Computer Simulation of Liquids*, Clarendon Press, Oxford, 1987, Chapter 5.
[17] Gallant, R. W. (1969). "Physical properties of hydrocarbons. XXXVI. Nitriles", *Hydrocarbon Process.*, **48**, 135.
[18] An, X. W. and Mansson, M. (1983). "Enthalpies of combustion and formation of acetonitrile", *J. Chem. Thermodyn.*, **15**, 287.
[19] Narayanaswamy, G., Dharmaraju, G. and Raman, G. K. (1981). "Excess volumes and isentropic compressibilities of acetonitrile, +*n*-propanol, +*i*-propanol, +*n*-butanol, +*i*-butanol and +cyclohexanol at 303.15 K", *J. Chem. Thermodyn.*, **13**, 327.
[20] Wagman, D. D., Evans, W. H., Parker, V. B., Schumm, R. H., Halow, I., Bailey, S. M., Churney, K. L. and Nuttal, R. L. (1982). "The NBS Tables of Chemical Thermodynamic Properties. Selected Values for Inorganic and C_1 and C_2 Organic Substances in SI Units", *J. Phys. Chem. Ref. Data Suppl.*, **11**(2).
[21] Anta, J. A., Lomba, E., Alvarez, M., Lombardero, M. and Martín, C. (1997). "Gas–Liquid coexistence properties from reference hypernetted chain theory for linear polar solvents", *J. Phys. Chem. B*, **101**, 1451.
[22] Radnai, T., Itoh, S. and Ohtaki, H. (1988). "Liquid structure of *N,N*-Dimethilformamide, acetonitrile, and their 1:1 molar mixture", *Bull. Chem. Soc. Jpn.*, **61**, 3845.
[23] Narten, A. H. (1979). "X-ray diffraction study of liquid neophentane in the temperature range −17 to 150°C", *J. Chem. Phys.*, **70**, 299.
[24] *International Tables for X-ray Crystallography* (The Kynoch Press, Birmingham, 1974), **4**, 99.
[25] Kovacs, H., Kowalewski, J., Maliniak, A. and Stilbs, P. (1989). "Multinuclear relaxation and NMR self-diffusion study of the nuclear dynamics in acetonitrile–chloroform liquid mixtures", *J. Phys. Chem.*, **93**, 962.
[26] Kunz, W., Calmettes, P. and Bellisent-Funel, M. C. (1993). "Dynamics of liquid acetonitrile at high frequencies", *J. Chem. Phys.*, **99**, 2079.
[27] Böhm, H. J., Lynden-Bell, R. M., Madden, P. A. and McDonald, I. R. (1984). "Molecular motion in a model of liquid acetonitrile", *Mol. Phys.*, **51**, 761.
[28] Yuan, P. and Schwartz, M. (1990). "Molecular reorientation in acetonitrile. A comparison of diffusion coefficients from Raman bandshapes and nuclear magnetic resonance relaxation times", *J. Chem. Soc. Faraday Trans.*, **86**, 593.
[29] Sugitani, A., Ikawa, S. and Konaka, S. (1990). "Effect of temperature on the infrared bandshapes and reorientational and vibrational relaxation of liquid acetonitrile", *Chem. Phys.*, **142**, 423.
[30] de Leeuw, S. W., Perram, J. W. and Smith, E. R. (1986). "Computer simulation of the static dielectric constant of systems with permanent electric dipoles", *Ann. Rev. Phys. Chem.*, **37**, 245.

[31] Flyvjberg, H. and Petersen, H. G. (1989). "Error estimates on averages of correlated data", *J. Chem. Phys.*, **91**, 461.
[32] Barthel, J., Kleebauer, M. and Buchner, R. (1995). "Dielectric relaxation of electrolyte solutions in acetonitrile", *J. Solution Chem.*, **24**, 1.
[33] Newmann, M., Steinhauser, O. and Pawley, G. S. (1984). "Consistent calculation of the static and frequency-dependent dielectric constant in computer simulations", *Mol. Phys.*, **52**, 97.
[34] Newmann, M. (1986). "Dielectric relaxation in water. Computer simulations with the TIP4P potential", *J. Chem. Phys.*, **85**, 1567.
[35] Martí, J., Guàrdia, E. and Padró, J. A. (1994). "Dielectric properties and infrared spectra of liquid water: Influence of the dynamic cross correlations", *J. Chem. Phys.*, **101**, 10883.
[36] Casulleras, J. and Guàrdia, E. (1992). "Computer simulation of liquid methanol II. System size effects", *Mol. Simul.*, **8**, 273.
[37] Tironi, I. G. and Van Gunsteren, W. F. (1994). "A molecular dynamics simulation study of chloroform", *Mol. Phys.*, **83**, 381.
[38] Madden, P. A. and Kivelson, D. (1984). "A consistent molecular treatment of dielectric phenomena", *Adv. Chem. Phys.*, **56**, 467.